Article

Full and Partial Deuterium Solvent Isotope Effect Studies of α-Thrombin-Catalyzed Reactions of Natural Substrates

Daoning Zhang, and Ildiko M. Kovach

J. Am. Chem. Soc., **2005**, 127 (11), 3760-3766• DOI: 10.1021/ja043258o • Publication Date (Web): 23 February 2005

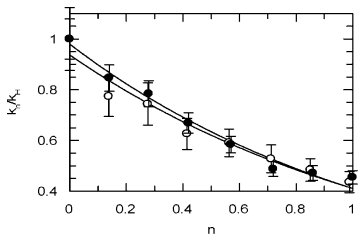

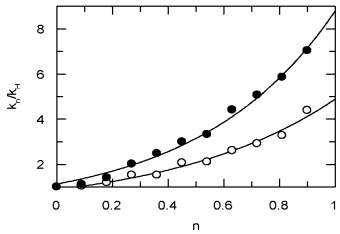

Fibrinogen→ FpA + fibrin1→ FpB + protofibril→ lateral polymer→ fibrin

More About This Article

Additional resources and features associated with this article are available within the HTML version:

- Supporting Information
- Access to high resolution figures
- Links to articles and content related to this article
- Copyright permission to reproduce figures and/or text from this article

View the Full Text HTML

J|A|C|S
ARTICLES
Published on Web 02/23/2005

Full and Partial Deuterium Solvent Isotope Effect Studies of α-Thrombin-Catalyzed Reactions of Natural Substrates

Daoning Zhang[§] and Ildiko M. Kovach*

Contribution from the Chemistry Department, The Catholic University of America, Washington D.C. 20064

Received November 9, 2004; E-mail: kovach@cua.edu

Abstract: Proton inventory studies of the thrombin-catalyzed fibrinogen activation to fibrinopeptide A are most consistent with a two-proton bridge forming at the transition state probably between Ser^{195} OγH and His^{57} Nϵ2 and His^{57} Nδ1 and Asp^{102} COOβ- at the active site, with fractionation factors 0.66 ± 0.03 under enzyme saturation with substrate and 0.64 ± 0.03 at fibrinogen concentration at 0.2 K_m, at pH 8.0, pD 8.6, and 25.0 ± 0.1 °C. Strongly inverse solvent isotope effects (SIEs) result from inverse lag times and maximal slopes of blood clotting plots, which are also anion and cation dependent. The blood clot is much coarser in D_2O, as indicated in clotting curves with 3−9 times shorter lag time and steeper slopes with respect to H_2O. The finer the particles, the weaker the H-bonds interlocking the fibrin mesh and/or in water structure around fibrin. Proton inventories of inverse lag times and maximal slopes of blood clotting curves in buffers containing Na^+ and Cl^- ions give the best fit to an exponential dependence on deuterium content in the buffer and give fractionation factors 5.6 ± 0.5 and 7.8 ± 0.6 at pH 8.0 and 25.0 ± 0.1 °C. The thrombin-catalyzed activation of protein C (PC) to APC is associated with inverse kinetic SIEs (KSIEs) of 0.75 ± 0.09 and 1.02 ± 0.06 in 0.3 M NaCl and 0.3 M choline chloride, respectively, at substrate concentrations = 0.2 K_m. In comparison, thrombin-catalyzed hydrolysis of chromogenic substrates gives greater KSIEs (Enyedy, E. I.; Kovach. I. M *J. Am. Chem. Soc.* **2004**, *126*, 6017−6024) and more complex proton inventories than the ones reported here for the first time for natural substrates. The present study illuminates differences in the character of the rate-determining transition state for the initial phase of the two physiological reactions catalyzed by thrombin.

Introduction

Thrombin (factor IIa) is one of the two best characterized of the serine protease enzymes in the cardiovascular system;[1−6] the other is factor Xa (FXa). Each enzyme performs a pivotal catalytic role in zymogen activation with optimal efficiency.[6−11] Activation involves the hydrolysis of one or two peptide bonds in a large precursor protein, using the general base catalytic apparatus of the protease. Biological general acid−base-catalyzed reactions[12] have been widely studied by deuterium kinetic solvent isotope effects (KSIEs)[13−17] to establish the occurrence of protonic bridges at the rate-determining transition state(s) (TSs). Additional information on the number and nature of proton bridges at the rate-determining TSs can be obtained from a broader analysis of partial solvent isotope effects or proton inventories measured in the mixtures of buffered water and heavy water.[13−23]

[§] Current address: Center for Biomolecular Structure & Organization, Department of Chemistry & Biochemistry, University of Maryland, College Park, MD 20742-3360.

(1) Furie, B.; Furie, B. C. *Cell* **1988**, *53*, 505−518.
(2) Davie, E. W.; Fujikawa, K.; Kisiel, W. *Biochemistry* **1991**, *30*, 10363−10370.
(3) Berliner, L. J. *Thrombin: Structure and Function*; Plenum Press: New York, 1992; pp 63−438.
(4) Mann, K. G.; Lorand, L. *Methods Enzymol.* **1993**, *222*, 1−10.
(5) Patthy, L. *Methods Enzymol.* **1993**, *222*, 10−22.
(6) Dang, Q. D.; Vindigni, A.; Di Cera, E. *Proc. Natl. Acad. Sci. U.S.A.* **1995**, *92*, 5977−5981.
(7) Stone, S. R.; Betz, A.; Hofsteenge, J. *Biochemistry* **1991**, *30*, 9841−9848.
(8) Vindigni, A.; Di Cera, E. *Biochemistry* **1996**, *35*, 4417−4426.
(9) Di Cera, E.; Dang, Q. D.; Ayala, Y.; Vindigni, A. *Methods Enzymol.* **1995**, *259*, 127−144.
(10) Di Cera, E.; Dang, Q. D.; Ayala, Y. M. *Cell Mol. Life Sci.* **1997**, *53*, 701−730.
(11) Pineda, A. O.; Savvides, S. N.; Waksman, G.; Di Cera, E. *J. Biol. Chem.* **2002**, *277*, 40177−40180.
(12) Fersht, A. *Structure and Mechanism in Protein Science*; W.H. Freeman, New York, 1999; pp 1−631.
(13) Alvarez, F. J.; Schowen, R. L. Mechanistic Deductions from Solvent Isotope Effects. In *Isotopes in Organic Chemistry*; Buncel, E., Lee, C. C., Eds.; Elsevier: Amsterdam, 1987; pp 1−60.
(14) Kresge, A. J.; More, O.; Powell, M. F. Solvent Isotopes Effects, Fractionation Factors and Mechanisms of Proton Transfer Reactions. In *Isotopes in Organic Chemistry*; Buncel, E., Lee, C. C., Eds.; Elsevier: Amsterdam, 1987; pp 177−273.
(15) Schowen, R. L. Structural and Energetic Aspects of Protolytic Catalysis by Enzymes: Charge−Relay Catalysis in the Function of Serine Proteases. In *Mechanistic Principles of Enzyme Activity*; Liebman, J. F., Greenberg, A., Eds.; VCH Publishers: New York, 1988; pp 119−168.
(16) Schowen, K. B.; Limbach, H. H.; Denisov, G. S.; Schowen, R. L. *Biochim. Biophys. Acta* **2000**, *1458*, 43−62.
(17) Quinn, D. M.; Sutton, L. D. Theoretical Basis and Mechanistic Utility of Solvent Isotope Effects. In *Enzyme Mechanism from Isotope Effects*; Cook, P. F., Ed.; CRC Press: Boston, MA, 1991; pp 73−126.
(18) Elrod, J. P.; Hogg, J. L.; Quinn, D. M.; Schowen, R. L. *J. Am. Chem. Soc.* **1980**, *102*, 5365−5376.
(19) Venkatasubban, K. S.; Schowen, R. L. *CRC Crit. Rev. Biochem.* **1985**, *17*, 1−44.
(20) Stein, R. L.; Elrod, J. P.; Schowen, R. L. *J. Am. Chem. Soc.* **1983**, *105*, 2446−2452.
(21) Stein, R. L.; Strimpler, A. M.; Hori, H.; Powers, J. C. *Biochemistry* **1987**, *26*, 1305−1314.
(22) Scholten, J. D.; Hogg, J. L.; Raushel, F. M. *J. Am. Chem. Soc.* **1988**, *110*, 8246−8247.
(23) Chiang, Y.; Kresge, A. J.; Chang, T. K.; Powell, M. F.; Wells, J. A. *J. Chem. Soc., Chem. Commun.* **1995**, 1587−1588.

10.1021/ja043258o CCC: $30.25

We have recently presented conclusions from the results and analysis of proton inventory data obtained on human-α-IIa-catalyzed hydrolysis of oligopeptide mimics of the respective natural substrates.[24] The extent and nature of P and P′ sites in effectors of IIa have a key role in mobilizing proton bridges at the rate-determining TS in acylation of the enzyme. Simple dipeptide amides invoke the participation of a single proton, while longer and more specific substrates recruit two or multiproton participation in the formation of proton bridges at the TS. This is in accord with the efficiency of peptide bond cleavage indicated by the magnitude of k_{cat}/K_m.[12,25] Schowen's hypothesis[13,15,18−21] that subsites on peptide substrates exert a compression to elicit contraction of the distance between proton donors and acceptors in acid−base catalytic pairs at the enzyme's active site has been confirmed by these IIa-catalyzed reactions. In IIa-catalyzed reactions, as in the pancreatic proteases, multiproton catalysis and includes one protonic bridge between Nϵ2 of His^{57} and OγH of Ser^{195} and one between Nδ1 of His^{57} and COOβ- of Asp^{102} at the active site.[12,24] ^{1}H NMR signals of short strong hydrogen bonds (SSHBs) forming at the active site in serine hydrolases,[26] including pancreatic proteases[27−31] and other enzymes,[32−35] when modified by mechanism-based inhibitors, have also been broadly studied and discussed. These SSHBs seem to be good models for proton transfer in the general acid−base-catalyzed steps that may also be mediated by a SSHB(s) at the TS.[16]

We have also shown that the hallmark of the effect of P′ residues in leaving group departure is a conformational change associated with a major rearrangement of solvate water. In IIa-catalyzed reactions, a net increase occurs in the isotopic fractionation factors for hydrogen bonds at solvation sites in the rate-determining step. This effect is elicited by interactions at the leaving group's binding site or substrate specificity site, which observation is well supported by other studies of P′ site interactions in catalysis[36−38] and inhibition[39] of proteases. The proton inventory technique, thus, proved to be very informative about the importance of solvent reorganization in substrate binding and leaving group release.

In light of the above and an increasing understanding of the critical role of water structure in enzyme kinetics,[40,41] it seemed to be a valuable endeavor to carry out KSIE and proton inventory studies on human-α-IIa-catalyzed reactions of natural substrates. Therefore, we carried out proton inventory experiments for the IIa-catalyzed activation of fibrinogen into fibrinopeptide A (FpA), the formation of fibrin colloid, and the IIa-catalyzed activation of protein C (PC) to activated protein C (APC). The proton inventories for FpA release in fibrinogen activation are bowl-shaped and are most consistent with two protonic bridges forming at the TS for acylation, at all substrate concentrations. This finding indicates that peptide cleavage rather than some physical step determines the rate of the first phase of the process. Inverse KSIEs and complex proton inventories observed on clotting curves are most consistent with the lateral polymerization of fibrin monomers being the dominant process under these conditions. The development of post-FpA-release turbidity is very dependent on the nature of cations and anions, which is consistent with differences in solvate water structure; this is further amplified in D_2O. The activation of PC gives KSIEs that are slightly inverse at substrate concentrations below K_m, indicating the dominance of physical rather than chemical steps limiting the rate under these conditions.

Experimental Section

Materials. Anhydrous dimethyl sulfoxide (DMSO), heavy water with 99.9% deuterium content, and anhydrous methanol were purchased from Aldrich Chemical Co. All buffer salts were reagent grade and were purchased from Aldrich, Fisher, or Sigma Chemical Co. Fibrinogen 56% pure (HPLC), fibrinopeptide A (FpA) 98% pure (HPLC), and fibrinopeptide B (FpB) 98% pure (HPLC) were purchased from Sigma Chemical Co. H-D-Phe-Pip-Arg-4-nitroanilide·HCl (*p*-NA) (S-2238) 99% (TLC) and Pyro-Glu-L-Pro-L-Arg-*p*-NA·HCl (S-2366) 99% (TLC) were purchased from Diapharma Group Inc. Human α-IIa, MM 36 500 d, 3010 NIH unit/mg activity in pH 6.5, 0.05 M sodium citrate buffer, 0.2 M NaCl and 0.1% PEG-8000, human PC, MM 62 000 d, 1.50 mg/mL in pH 7.4, 0.02 M Tris−HCl buffer, 0.1 M NaCl and 1 mM benzamidine, and human APC, MM 56 000 d, 1.19 mg/mL in pH 7.4, 0.02 M Tris buffer and 0.1 M NaCl were purchased from Enzyme Research Laboratories. Rabbit thrombomodulin (TM), MM 74 000 d, 4.7 mg/mL in TBS buffer, 0.05% PDOC, 0.02% NaN_3 was purchased from Hematologic Technologies Inc. r-Hirudin 2000 antithrombin units were purchased from Centerchem Inc.

Instruments. Quantitative HPLC analysis of IIa-catalyzed fibrinogen hydrolysis was performed using a Waters HPLC system, Waters Delta PAK C18 300A 150 × 3.9 mm column, and Phenomenex Bondalone C18 10μ 300 × 3.9 mm column. Spectroscopic measurements were performed with a Perkin-Elmer Lambda 6 UV−vis spectrophotometer as described previously.[24]

Solutions. Buffers were prepared by weight from Tris−base and Tris−HCl in the range of pH 7.1−9.1 in freshly distilled deionized water or heavy water that contained 0.02 M Tris, 0.005−0.30 M NaCl, 0.1% PEG-4000, and either choline chloride (ChCl) or $CaCl_2$, also described previously.[24]

Active Site Titrations. To determine the concentration of IIa, 490 μL of 64 μM S-2238 substrate solution was incubated at 25.0 ± 0.1 °C. The titration was initiated by adding 10 μL of IIa solution. Initial rates of substrate hydrolysis were measured by monitoring the release of *p*-nitroaniline at 405 nm for 30 s. The same stock solution was used for all experiments on the same day with intermittent checking of activity. There was no background hydrolysis of the substrates in the absence of enzyme, and the slopes were proportional to IIa concentration within 90% of the values calculated from weights.

Quantitative HPLC Analysis. The release of FpA from fibrinogen hydrolysis was monitored using an isocratic HPLC method. The optimal

(24) Enyedy, E. J.; Kovach, I. M. *J. Am. Chem. Soc.* **2004**, *126*, 6017−6024.
(25) Hedstrom, L. *Chem. Rev.* **2002**, *102*, 4501−4524.
(26) Mildvan, A. S.; Massiah, M. A.; Harris, T. K.; Marks, G. T.; Harrison, D. H. T.; Viragh, C.; Reddy, P. M.; Kovach, I. M. *J. Mol. Struct.* **2002**, *215*, 163−175.
(27) Frey, P. A.; Whitt, S. A.; Tobin, J. B. *Science* **1994**, *264*, 1927−1930.
(28) Tobin, J. B.; Whitt, S. A.; Cassidy, C. S.; Frey, P. A. *Biochemistry* **1995**, *34*, 6919−6924.
(29) Cassidy, C. S.; Lin, J.; Frey, P. A. *Biochemistry* **1997**, *36*, 4576−4584.
(30) Lin, J.; Westler, W. M.; Cleland, W. W.; Markley, J. L.; Frey, P. A. *Proc. Natl. Acad. Sci. U.S.A.* **1998**, *95*, 14664−14668.
(31) Lin, J.; Cassidy, C. S.; Frey, P. A. *Biochemistry* **1998**, *37*, 11940−11948.
(32) Halkides, C. J.; Wu, Y. Q.; Murray, C. J. *Biochemistry* **1996**, *35*, 15941−15948.
(33) Ash, E. L.; Sudmeier, J. L.; De Fabo, E. C.; Bachovchin, W. W. *Science* **1997**, *278*, 1128−1132.
(34) Kahayaoglu, A.; Haghjoo, K.; Guo, F.; Jordan, F.; Kettner, C.; Felfoldi, F.; Polgar, L. *J. Biol. Chem.* **1997**, *272*, 25547−25554.
(35) Bao, D.; Huskey, P. W.; Kettner, C. A.; Jordan, F. *J. Am. Chem. Soc.* **1999**, *121*, 4684−4689.
(36) Schellenberger, V.; Turck, C. W.; Rutter, W. J. *Biochemistry* **1994**, *33*, 4251−4257.
(37) Schellenberger, V.; Turck, C. W.; Hedstrom, L.; Rutter, W. J. *Biochemistry* **1993**, *32*, 4349−4353.
(38) Le Bonniec, B. F.; Myles, T.; Johnson, T.; Knight, C. G.; Tapparelli, C.; Stone, S. R. *Biochemistry* **1996**, *35*, 7114−7122.
(39) Dai, Y.; Hedstrom, L.; Abeles, R. H. *Biochemistry* **2000**, *39*, 6498−6502.
(40) Park, C.; Raines, R. T. *J. Am. Chem. Soc.* **2001**, *123*, 11472−11479.
(41) Ru, M. T.; Hirokane, S. Y.; Lo, A. S.; Dordick, J. S.; Reimer, J. A.; Clark, D. S. *J. Am. Chem. Soc.* **2000**, *122*, 1565−1571.

eluting solvent composition was determined as 78% of 0.1% trifluoroacetic acid (TFA) and 22% acetonitrile (CH_3CN). The optimal flow rate was 0.7 mL/min; the injection volume was 20 μL, and the detection wavelength was 205 nm. External standards were used to establish the correlation of the signal response to concentration (0.001−0.1 mg/mL) and detection limit of FpA.

For initial rate studies and for pseudo-first-order-rate studies, 0.55−33 μM and 0.55 μM fibrinogen solutions in 1 mL, respectively, were mixed with 10 μL of 8 nM IIa solution at pH 8.0, 0.30 M NaCl, and 25.0 ± 0.1 °C. At different time intervals, a 100 μL reaction mixture was transferred to a microtube and quenched by 3.2 μL of 9.3 M $HClO_4$. The quenched reaction mixture was centrifuged at 4000 × g for 20 min. A 70 μL aliquot of the supernatant was transferred to a microtube and subjected to HPLC analysis.

Turbidity Study of Fibrinogen Activation. Fibrinogen solution at 1.1 μM was prepared, and 495 μL of it was incubated in a UV−vis cuvette at pH 8.0, 0.30 M NaCl, and 25.0 ± 0.1 °C for 15 min before it was mixed with 5 μL of a 150 nM IIa solution to start the reaction. Light scatter was recorded at 350 nm.

Calibration Curve Construction for APC Activity. APC solutions were prepared in concentrations ranging from 0.2 to 10 nM. Ten microliters of S-2366 solution was added to 490 μL of APC solution to a final concentration of 200 μM at pH 8.5, 0.30 M NaCl, and 25.0 ± 0.1 °C. Initial rates of released *p*-NA were determined at known APC concentrations, and a rate versus concentration calibration curve was constructed.

Hirudin Effect on APC and IIa-Catalyzed S-2366 Hydrolysis. Fifty microliter aliquots of 3.6 nM APC or 15 nM IIa solution were incubated with 0, 5, 10, and 15 μL of 44 units/mL hirudin at pH 8.5, 0.30 M NaCl, and 25.0 ± 0.1 °C for 15 min. Fifty microliters of the quenched solution was then transferred to a quartz cuvette containing 450 μL of 200 μM solution of the amidolytic S-2366 substrate preincubated at 25.0 ± 0.1 °C. The release of *p*-NA was monitored at 405 nm.

PC Activation by Human α-IIa. For PC activation, 300 nM IIa, 2 μM TM, 8 μM PC, and 44 units/mL hirudin were prepared using the pH 8.5 buffer. Then, 200 nM PC was incubated with 15 nM IIa in the presence of 100 nM TM in pH 8.5 buffer, 0.30 M NaCl or 0.30 M ChCl, 5 mM $CaCl_2$, and 0.1% PEG-4000 at 37.0 ± 0.1 °C. At predetermined time intervals, 50 μL of the reaction mixture was transferred to a polyethylene microtube and quenched by 10 μL of 44 units/mL hirudin. IIa is 99% inhibited under these conditions, while APC activity remains intact. To determine the concentration of released APC, 50 μL of the quenched reaction mixture was added to a 500 μL quartz cuvette containing 450 μL of 200 μM S-2366 substrate solution at 25.0 ± 0.1 °C. Initial rates of substrate hydrolysis were measured by monitoring the release of *p*-NA at 405 nm for 30 s. The concentration of APC was determined by reference to a standard curve.

Proton Inventory Experiments. Experiments were performed at pH 8.0−8.5 and equivalent pL in isotopic buffers at $n = 0-1$ using either initial rates or at $[S] \ll K_m$ under pseudo-first-order conditions, in three repetitions.

Analysis of Kinetic and Proton Inventory Data. All data reductions using predefined and custom-defined equations were performed using the GraFit 3.3 software.[42]

Results

Standard Curves for FpA Appearance and APC Appearance. The response of the HPLC detector to FpA concentrations in the range of 0.001−0.1 mg/mL (Figure 1S in the Supporting Information) was linear. The detection limit at 2-fold baseline noise was determined to be 0.0005 mg/mL, equivalent to 0.325 μM.

(42) Leatherbarrow, R. J. *GraFit User's Guide*; Ertihacus Sofware Ltd.: Staines, U.K., 1992.

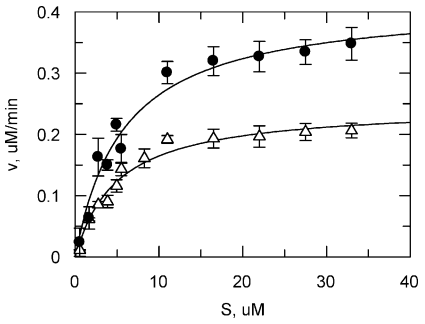

Figure 1. Michaelis Menten study of FpA release during IIa-catalyzed fibrinogen hydrolysis in 0.02 M Tris buffer, pH 8.0, containing 0.30 M NaCl, 0.1% PEG, and 0.08 nM IIa at 25.0 ± 0.1 °C. Circles represent H_2O buffer, and triangles represent D_2O buffer ($n = 0.99$).

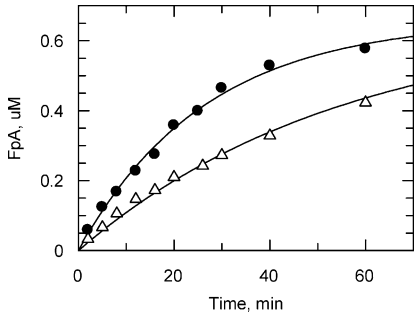

Figure 2. Pseudo-first-order kinetics for fibrinogen activation catalyzed by IIa; conditions and symbols are indicated in Figure 1. The errors are smaller than the symbols.

APC concentration between 0.2 and 10 nM gave a linear response to the absorbance change at 405 nm due to *p*-NA release from S-2366. The best fit of the correlation curve gave [APC] in nM = $\Delta Abs_{405}/s \times 643$, $R^2 = 0.9962$.

Fibrinogen Activation. Initial rate data of FpA release during IIa-catalyzed fibrinogen hydrolysis are displayed in Figure 1. The K_m value of IIa-catalyzed fibrinogen hydrolysis is 5.8 ± 1.0 μM in H_2O buffer, in agreement with the published value of 5.7 ± 0.5 μM.[8] The K_m value is 5.0 ± 0.7 μM in D_2O buffer. V_{max} at 0.08 nM IIa at 25.0 ± 0.1 °C was determined to be (7.0 ± 0.3) × 10^{-9} M s^{-1} and $k_{cat} = 75 \pm 5$ s^{-1} in H_2O buffer, and V_{max} is (2.4 ± 0.2) × 10^{-9} M s^{-1} and $k_{cat} = 35 \pm 2.5$ s^{-1} in D_2O buffer. The first-order release of FpA in pH 8.0 Tris buffer is shown in Figure 2. The rate constants were calculated to be (6.50 ± 0.15) × 10^4 s^{-1} in H_2O buffer and (3.00 ± 0.07) × 10^4 s^{-1} in 99% D_2O buffer at 0.08 nM IIa concentration, giving $k_{cat}/K_m = (8.0 \pm 0.2) \times 10^6$ M^{-1} s^{-1} in H_2O and (4.08 ± 0.10) × 10^6 M^{-1} s^{-1} in 99% D_2O, which are within 2-fold of the values calculated from initial rates.

Model Selection for the Evaluation of Proton Inventory Data. As detailed previously,[24] we developed a protocol for using variations on the Gross−Butler equation,[13,14,19,49,50] which is given below (eq 1). It relates the dependence of a particular rate parameter to the atom fraction of deuterium, *n*, in the solvent mixtures:

$$V_n = V_o \prod_i^{TS} (1 - n + n\phi^T{}_i) / \prod_j^{RS} (1 - n + n\phi^R{}_j) \qquad (1)$$

where V_n and V_o are velocities (or rate constant) in a binary solvent and in water, respectively, n = atom fraction of deuterium, RS = reactant state, ϕ^R = RS fractionation factor,

Chart 1. Models for Fitting Proton Inventory Data

Information obtained	Equation
TS_1	$V_n = V_H (1 - n + n\,\phi_1)$
TS_1, solv.	$V_n = V_H (1 - n + n\,\phi_1)\,\phi_S^n$
$2TS_1$	$V_n = V_H (1 - n + n\,\phi_1)^2$
$2TS_1$, solv.	$V_n = V_H (1 - n + n\,\phi_1)^2 \phi_S^n$
TS_1, TS_2	$V_n = V_H (1 - n + n\,\phi_1)(1 - n + n\,\phi_2)$
TS_1, TS_2, solv.	$V_n = V_H (1 - n + n\,\phi_1)(1 - n + n\,\phi_2)\,\phi_S^n$

and ϕ^T = TS fractionation factor. The fractionation factors are basically inverted equilibrium isotope effects, K_D/K_H, for exchange between a bulk water site and a particular structural site of the RS or the TS. The most common simplifications of this equation involve the assumption of a unit fractionation factor of RSs for catalytic residues with NH and OH functional groups and the assumption that one or two active-site units contribute in most hydrolytic enzymes. Models that gave reasonable fit and were deemed feasible in this study are given in Chart 1.We calculated a single exponential term for a generalized solvent rearrangement,[14,23] symbolized by ϕ_S^n, regardless its origin, as best justified by past evidence.[24,51] Least-squares fitting to the different models yields the contributing ϕ^T_i and ϕ^R_i, that is, isotope effects along with the reduced χ^2 values. The model giving the best statistical result and fractionation factors consistent with a sensible mechanism for both k_{cat} and k_{cat}/K_m data was used for calculating the line.

The proton inventory plots for fibrinogen activation at concentrations at 0.2 and 5 K_m are presented in Figure 3. (Numerical data are provided in the Supporting Information, Tables 1S−3S.)

Figures 4 and 5 give representative plots for the turbidity study of fibrin formation in the presence of F^-, Cl^-, Na^+, choline cation (Ch^+), and Ca^{2+} in H_2O and D_2O.

Blood clotting curves were analyzed in past studies for the lag time at the outset, the maximal slope along the ascent of the curve, and the final absorbance.[8,43−48] The lag time was claimed to be correlated with protofibril formation, and the maximal slope (V_{max}) was claimed to report on the rate of lateral aggregation of protofibrils.[46−48] The final absorption is related to the thickness of the fibers.[46−48] The lag times and maximal slopes of the curves in Figures 4 and 5 were calculated and are tabulated, along with the solvent isotope effects (SIEs) obtained from them, in Table 1. The effect of cations and anions in H_2O and D_2O are tabulated in Table 2.

(43) Larsson, U. *Eur. J. Biochem.* **1988**, *174*, 139−144.
(44) De Cristofaro, R.; Di Cera, E. *J. Protein Chem.* **1991**, *10*, 455−468.
(45) De Cristofaro, R.; Di Cera, E. *Biochemistry* **1992**, *31*, 257−265.
(46) Mullin, J. L.; Gorkun, O. V.; Lord, S. T. *Biochemistry* **2000**, *39*, 9843−9849.
(47) Lounes, K. C.; Ping, L.; Gorkun, O. V.; Lord, S. T. *Biochemistry* **2002**, *41*, 5291−5299.
(48) Kostelansky, M. S.; Lounes, K. C.; Ping, L. F.; Dickerson, S. K.; Gorkun, O. V.; Lord, S. T. *Biochemistry* **2004**, *43*, 2475−2483.
(49) Gold, V. *Adv. Phys. Org. Chem.* **1969**, *7*, 259−331.
(50) Kresge, A. J. *Pure Appl. Chem.* **1964**, *8*, 243−258.
(51) Stein, R. L. *J. Am. Chem. Soc.* **1985**, *107*, 6039−6042.

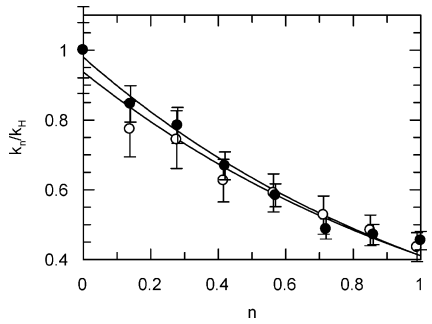

Figure 3. Proton inventory for the IIa-catalyzed fibrinogen hydrolysis; conditions are indicated in Figure 1. The initial rate data at 22 μM fibrinogen concentration are symbolized by open circles, and the equation of the line is $k_n/k_H = 0.90\ (1 - n + n/1.51)$.[2] Pseudo-first-order data at 0.55 μM fibrinogen concentration are symbolized by filled circles, and the equation of the line is $k_n/k_H = 0.98\ (1 - n + n/1.56)$.[2]

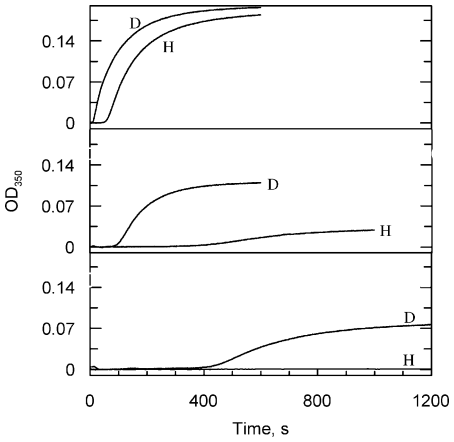

Figure 4. Time course of turbidity development during fibrin formation from 0.33 μM fibrinogen, catalyzed by 1.5 nM IIa at conditions indicated in Figure 1 in H_2O on the lower curve and D_2O ($n = 0.88$) on the upper curve of each graph: (top) in the presence of 0.30 M NaF; (middle) in the presence of 0.30 M NaCl; and (bottom) in the presence of 0.30 M ChCl.

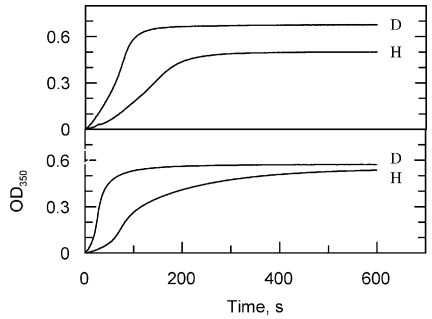

Figure 5. Time course of turbidity development during fibrin formation; conditions are as indicated in Figure 4: (top graph) in the presence of 0.30 M ChCl and 5 mM $CaCl_2$; (bottom graph) in the presence of 0.30 M NaCl and 5 mM $CaCl_2$.

The dependence of the inverse lag time, analogous to first-order rate constants, and the maximal slope of turbidity plots acquired in mixtures of buffered H_2O and D_2O give deeply curved profiles that fit exponential dependence on n, atom fraction D content in the buffer, exemplified by Figure 6.

Activation of PC. IIa-catalyzed PC activation was carried out at 0.02 K_m for PC and at IIa concentrations of 5.8 and 13.1 nM and in the presence of 0.30 M NaCl; the reaction was complete after 120 and 50 min of incubation, respectively. Control experiments proved that hirudin effectively quenches the activity of IIa (99%) while leaving APC activity intact under

Table 1. Maximal Slopes, Lag Time, and SIEs Obtained from Clotting Curves Shown in Figures 4 and 5

salt	isotopic water	max slope (SI) 10^3 OD/s	lag time (τ) s	KSIE (corrected for 100% D) SI_H/SI_D	KSIE (corrected for 100% D) $1/\tau_H/1/\tau_D$
NaF	H	1.42 ± 0.01	59	0.563 ± 0.005	0.18
	D	2.39 ± 0.02	12		
NaCl	H	0.17 ± 0.02	347	0.129 ± 0.015	0.21
	D	1.18 ± 0.02	79		
ChCl	H	0.028 ± 0.002		0.103 ± 0.010	
	D	0.26 ± 0.02	427		
NaCl, $CaCl_2$	H	3.21 ± 0.02		0.305 ± 0.003	
	D	9.66 ± 0.06			
ChCl, $CaCl_2$	H	5.27 ± 0.02		0.251 ± 0.003	
	D	19.08 ± 0.24			

Table 2. Ion Effect on Maximal Slopes Obtained from Clotting Curves in Figures 4 and 5

	salt x/y	SI_x/SI_y in H_2O	SI_x/SI_y in D_2O ($n = 0.88$)
anion effect	NaF/NaCl	8.4 ± 1.0	2.03 ± 0.04
cation effect	NaCl/ChCl	5.7 ±0.8	4.6± 0.4
	NaCl, $CaCl_2$/NaCl	18.9 ± 2.3	8.2 ± 0.2
	ChCl, $CaCl_2$/ChCl	177 ± 13	73 ± 6
	NaCl, $CaCl_2$/ChCl, $CaCl_2$	0.610± 0.005	0.51 ± 0.01

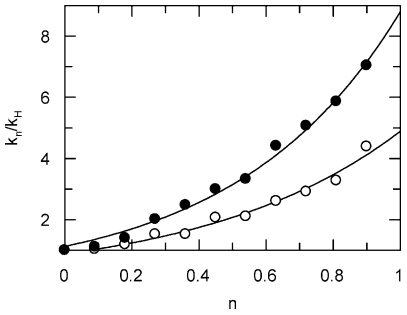

Figure 6. Proton inventory for the development of turbidity during fibrin formation at conditions indicated in Figure 1. Open circles represent inverse partial solvent isotope effects for the inverse lag (life) time, and the line was calculated from $1/\tau_n/1/\tau_H = 0.88(\pm0.06)\ [5.55(\pm0.52)]^n$. Closed circles are for the maximal slopes of turbidity plots, and the line was calculated from $SI_n/SI_H = 1.13(\pm0.06)\ [7.79(\pm0.56)]^n$. Errors were smaller than the diameter of the circles.

these experimental conditions. KSIE data at 13.1 nM IIa are presented in Figure 7. The curves for the reaction at 0.30 M ChCl are in Figure 8, and the isotope effect is near unity. The data are summarized in Table 3.

Discussion

Human α-IIa-Catalyzed Fibrin Formation. The pivotal reaction in blood clotting is the IIa-catalyzed hydrolysis of two peptide bonds in fibrinogen, which generate fibrin monomers that further interlock into a fibrin mesh, according to Scheme 1.[6,8,52]

IIa binds to fibrinogen in the central amino-terminal region and cleaves FpA and FpB from the Aα and Bβ chains, respectively. Polymerization occurs after FpA is released from fibrinogen. FpB release occurs more slowly than the release of FpA and is thought to concur with, and enhance, lateral growth and/or branching of the protofibril.[46−48]

(52) Pineda, A. O.; Carrell, C. J.; Bush, L. A.; Prasad, S.; Caccia, S.; Chen, Z. W.; Mathews, F. S.; Di Cera, E. *J. Biol. Chem.* **2004**, *279*, 31842−31853.

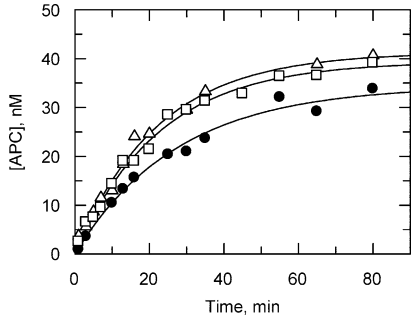

Figure 7. Solvent isotope effect for IIa-catalyzed PC activation at pH 8.5 in 0.02 M Tris, 0.30 M NaCl, 5 mM $CaCl_2$, 0.1% PEG-4000, 100 nM TM, 13.1 nM human IIa, and 37.0 ± 0.1 °C. Circles represent H_2O buffer, triangles D_2O buffer ($n = 0.91$), and square H_2O/D_2O buffer ($n = 0.45$). The errors are smaller than the symbols.

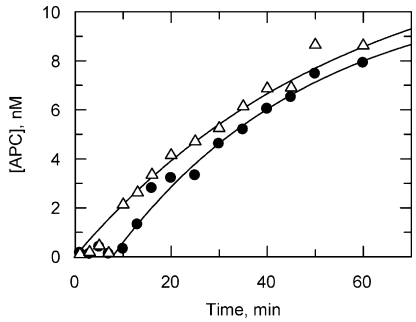

Figure 8. Solvent isotope effect for IIa-catalyzed PC activation at pH 8.5 in 0.02 M Tris, 0.3 M ChCl, and 5 mM $CaCl_2$. Other conditions and symbols are as described in Figure 7.

Table 3. Solvent Isotope Effects (calculated for 100% D) for IIa-Catalyzed PC Activation at pH 8.5 in 0.02 M Tris, 0.3 M NaCl/ChCl, 5 mM $CaCl_2$, 100 nM TM, and 0.1% PEG-4000, at 37.0 ± 0.1 °C

	$10^4\ k_H$, s^{-1}	$10^4\ k_{n=0.45}$, s^{-1}	$10^4\ k_D$, s^{-1}	^{DOD}k
NaCl, 5.8 nM IIa	2.80 ± 0.15		3.55 ± 0.17	0.79 ± 0.06
NaCl, 13.1 nM IIa	6.0 ± 0.7	7.42 ± 0.33	8.01 ± 0.33	0.75 ± 0.09
ChCl, 13.1 nM IIa	3.0 ± 0.2		2.95 ± 0.07	1.02 ± 0.06

Scheme 1

$$\text{Fibrinogen} \rightarrow \text{FpA} + \text{fibrin1} \rightarrow \text{FpB} + \text{protofibril} \rightarrow \text{lateral polymerization} \rightarrow \text{fibrin mesh}$$

Kinetics of the first two steps of the reaction have recently been studied in laboratory experiments, and the Michaelis Menten constants have been determined under various conditions using HPLC similar to the technique that we used.[8] However, reproducible detection of FpB, emerging ∼15 min after FpA, has been difficult in earlier studies as in our experience, and thus we abandoned it. Full IIa activity in catalyzing fibrinogen activation requires Na^+ concentrations at 0.30 M under laboratory conditions. The Michaelis Menten constants are in general agreement with those published earlier for the generation of FpA under similar conditions. The KSIE is moderate at 2.3 ± 0.2 for both k_{cat} and k_{cat}/K_m, and the proton inventory is bowl-shaped. The reduced χ^2 values are very close for a model with $\phi_1 = \phi_2 = 0.64 \pm 0.02$ for k_{cat}/K_m and 0.66 ± 0.03 for k_{cat} for two proton bridges occurring at the TS of the rate-determining step and for one with $\phi_1 = 1.01 \pm 0.04$ and $\phi_S = 0.41-0.43\ (\pm0.16)$ for both k_{cat} and k_{cat}/K_m. However, the standard deviations are decidedly the lowest for the two-

site model. Substrate mimics of fibrinogen give fractionation factors 0.50−0.68 for the two-site model, with very small solvent contributions.[24] On the basis of these observations, we propose that the occurrence of two-proton bridges at the TS for acylation involving the catalytic Ser and His is the most likely explanation for the data.

From our earlier study,[24] the data for tripeptide amides with Pro, Val, or Pip in the S_2 site also fit bowl-shaped curves, exemplified by N-t-Boc-Val-Pro-Arg-7-AMC; $\phi^{TS}{}_1 = \phi^{TS}{}_2 = 0.57 \pm 0.01$ and $\phi_S = 1$ for k_{cat} and 1.6 ± 0.1 for k_{cat}/K_m. Proton inventories for a nonapeptide, an internally fluorescence-quenched optimal sequence, (AB)Val-Phe-Pro-Arg-Ser-Phe-Arg-Leu-Lys(DNP)-Asp-OH, are linear, possibly due to some cancellation of normal and inverse effects. The data for k_{cat} for H-D-Phe-L-Pip-Arg-*p*-NA and an internally quenched decapeptide recognition sequence for factor VIII, (AB)Val-Ser-Pro-Arg-Ser-Phe-Gln-Lys(DNP)-Asp-OH, are most consistent with two identical fractionation factors for catalytic proton bridging, $\phi^{TS}{}_1 = \phi^{TS}{}_2 = 0.68 \pm 0.02$, and a large inverse component ($\phi_S = 3.1 \pm 0.5$) for the latter, indicative of substantial solvent reorganization, presumably upon departure of the Ser-Phe_Gln-Lys(DNP)-Asp-OH fragment. Proton inventory curves for k_{cat}/K_m for nearly all substrates are dome-shaped with an inverse isotope effect component ($\phi_S = 1.2-2.4$) originating from solvent reorganization during association of thrombin with substrate. Clearly, proton inventories for the IIa-catalyzed hydrolysis of this range of substrate mimic peptides present a range of complexities. The KSIEs and fractionation factors for fibrinogen hydrolysis are probably closest to the those for the decapeptide, except for the absence of solvent reorganization in the rate-determining step for fibrinogen cleavage to fibrin 1 and FpA and the release of FpA. The rate-determining event is probably amide bond cleavage in fibrinogen at both low and high saturation of IIa with fibrinogen. Vindigni and Di Cera came to the same conclusion on the basis of thermodynamic studies of IIa-catalyzed hydrolysis of fibrinogen.[8]

A unique result is the very strongly inverse SIE for the turbidity test for blood coagulation in the presence of Na^+ or Cl^-. The experiment yields information on the second bond cleavage and/or an associated conformational change, which is ensued by a physical phenomenon, lateral polymerization.[46−48] Intermolecular H-bonds are considered a main force in lateral polymerization in fibrin.[43] In other systems, polymerization has been reported to occur with great solvent rearrangement and strongly inverse KSIE.[53] Prior to or concurrent with lateral polymerization, a major conformational change occurs as the FpB peptide fragment is cleaved off.[48] Inverse KSIE characterizes this step as well, indicating a rate-determining conformational change rather then rate-determining bond cleavage. The systematic proton inventory study constructed from the inverse lag times and maximal slopes of blood clotting curves in mixed isotopic buffers resulted in concave curves and large fractionation factors for solvent rearrangement. This result is also corroborated by a great dependence of the blood coagulation curves on the specific anion or cation. Ion effects in H_2O are greater than those in D_2O (Table 2), especially with F^- and Ca^{2+}. We found, as did Vindigni and Di Cera,[8] that in the presence of F^- ions, the clot is thicker than in the presence of Cl^- ions. Also, the thickness of the clot decreases in the presence of cations in the following order: $Ca^{2+} > Na^+ > Ch^+$. The inverse KSIE is amplified greatly in the presence of Cl^- and Na^+, which generally cause the formation of finer precipitate in water, but D_2O greatly counteracts this effect. Both the lag time and the maximal slope of the blood clotting curve depend on the ion-perturbed water structure as indicated by the ion dependence. Structural changes in blood clot are associated with substantial changes in water structure affecting a net decrease in the strength of H-bonds as finer particles form. The KSIE becomes increasingly inverse with increasing substrate concentration as well, indicating either an increase in the number and/or strength of interlocking H-bonds or a tightening of the water structure around the lateral fiber formed as the concentration increases.

It has been reported that the bimolecular rate constant for the formation of FpA correlates with the lag time and the slope of the blood clotting curve.[8,44,45,52] However, KSIEs and proton inventories on the kinetics of FpA formation and the ensuing coagulation are very different, reflecting on different rate-determining steps for the two. The all-solvation model gives large fractionation factors for polymerization, which can be best understood as a conglomerate of many small sites contributing with inverse KSIE as the blood clot becomes coarser in D_2O.

Human α-IIa-Catalyzed Activation of Protein C. The other critical physiological function of IIa is the activation of PC to APC, which is a key thrombolytic enzyme, arresting blood coagulation.[6,54] We studied the reaction in the presence and absence of Na^+ ions, but always in the presence of TM and Ca^{2+} ions, as indicated in Table 3. In contrast to the initial phase of fibrinogen activation, two sets of reactions indicate inverse KSIE when IIa is in its fast form at Na^+ concentration, 0.30 M.[6,52] In the absence of Na^+ ions and at IIa concentration of 13.1 nM, the rate constants are about one-half of those at $[Na^+] = 0.30$ M, and a lag time is perceptible. Due to its complexity, the mechanism of PC activation has not been studied in depth yet, but the consistently inverse KSIEs seem to indicate a rate-determining physical step at PC concentrations below K_m. The KSIE is more inverse in the presence of Na^+ ion than in the presence of Ch^+ ion, which may again be related to cation effect on water structure during association of IIa with PC, a very large substrate. At the moment, the price of PC is prohibitive to a detailed study of the reaction under substrate saturation of IIa.

In conclusion, the proton inventory results on the release of FpA are most consistent with two protons transferring at the rate-determining acylation of IIa by fibrinogen. This result is similar to that with substrate mimics, but it is also simpler than proton inventories obtained with some internally fluorescence-quenched nona- and decapeptide mimics of the natural substrates. The strongly inverse KSIE and large fractionation factors obtained from the inverse lag time and the maximal slopes of blood clotting curves most likely report on either a conformational change associated with bond cleavage to FpB and/or the concurrent lateral polymerization. Both of these steps involve

(53) Harmony, J. A. K.; Himes, R. H.; Schowen, R. L. *Biochemistry* **1975**, *14*, 5379−5386.

(54) Cote, H. C. F.; Bajzar, L.; Stevens, W. K.; Samis, J. A.; Morser, J.; MacGillivray, R. T. A.; Nesheim, M. E. *J. Biol. Chem.* **1997**, *272*, 6194−6200.

rearrangement of H-bonds in the fibrin mesh and a major restructuring of solvate water, which is greatly dependent on the character of cations and anions present. The IIa-catalyzed activation of PC is associated with a slightly inverse KSIE, which indicates a physical step determining the rate of the early reaction at low substrate concentration. This study then illuminates differences in the character of the rate-determining TS for the initial phase of the two physiological reactions catalyzed by IIa.

Acknowledgment. We gratefully acknowledge the financial support of this research from the U.S. National Institute of Health, Grant No. 1 R15 HL067754-01.

Supporting Information Available: Two standard curves, seven tables of kinetic rate constants, and their ratios for proton inventories. This material is available free of charge via the Internet at http://pubs.acs.org.

JA043258O